CFD-based Optimization of Gas/Liquid Microreactors with Droplet and Bubble Transport

S. Hardt, H. Pennemann and F. Jiang

Institut für Mikrotechnik Mainz (IMM)
Carl-Zeiss-Str. 18-20, 55129 Mainz, Germany, hardt@imm-mainz.de

ABSTRACT

Two different concepts of gas/liquid microreactors are evaluated using methods of computational fluid dynamics. For the first design, an arrangement of parallel plates with functionalized surfaces, a method of droplet formation is suggested. Furthermore, the simulations show that the shape of the droplets transported by the gas flow strongly depends on the wettability of the surface. Surfaces with good wetting properties or high gas velocities result in droplets being disrupted while they are moving. The second concept is based on regular arrangements of bubbles being transported through a capillary. Experiments indicate that a small hydrodynamic dispersion is achieved with corresponding flow patterns. The experiments are supported by simulations, which show that bubbles keep their staggered arrangement while moving through a capillary. Both concepts promise to open up new directions towards high-performance gas/liquid microreactors with a narrow residence-time distribution and efficient mass transfer between the phases.

Keywords: Free-surface flow, volume-tracking method, gas/liquid microreactors, droplet and bubble dynamics.

1 INTRODUCTION

The economic figure of merit of chemical processes is, among other factors, closely interlinked with the conversion, yield and selectivity achieved in the corresponding reactions. It was shown that due to the high heat and mass transfer coefficients obtained in microchannels a superior performance of gas/liquid microreactors is obtained as compared to standard macroscopic processes [1]. Besides an efficient heat and mass transfer, a narrow residence-time distribution is a prerequisite for highly efficient processes, especially those that involve undesired side reactions. In a previous publication [2] the problem of hydrodynamic dispersion was studied for microreactors with layers of liquid and gas flow, using methods of computational fluid dynamics (CFD). Besides layered flow patterns there are two other possibilities for contacting a liquid and a gas phase: the transport of droplets surrounded by a gaseous medium and bubble flow. These two options are studied in the present article, with a special focus on finding configurations optimized for practical applications in micro process technology.

2 MATHEMATICAL MODELS

Almost inevitably multi-phase flow problems in microchannel geometries require the use of CFD methods for free-surface flow. A popular class of models is based on volume tracking by assigning a "color" value of either 0 or 1 to each of the phases. In order to describe the time evolution of the free-surface flow, a convection equation for the color field is solved. A direct solution of the corresponding transport equation in combination with the Navier-Stokes equation usually suffers from discretization errors inducing artificial diffusive fluxes, thus yielding a blurred interface and finally an unphysical equidistribution of the two phases. In order to avoid such artifacts, a special method, the so-called surface sharpening algorithm [3], was invented. In the framework of this approach each time step is followed by a correction step transferring matter to the other side of the interface. As an alternative to the direct solution of the convection equation for the color field, the volume-of-fluid (VOF) approach was developed [4]. Within this method a cell updating scheme for the evolution of the color field and a reconstruction scheme of the interface shape within computational cells is used. Due to explicit reconstruction of the interface, difficulties with numerical diffusion are avoided.

Each of these two methods has its specific advantages and drawbacks. The direct approach is computationally comparatively inexpensive and allows large time steps with Courant-Friedrich-Levy (CFL) numbers of about one or even larger. However, the surface-sharpening algorithm only ensures global mass conservation, while local mass conservation might be violated. The VOF method does not require a correction algorithm and thus allows for local mass conservation. However, it is computationally more demanding than the direct solution method. In addition to that, the CFL number is limited to values significantly smaller than one, thus severely constraining the time-step size.

The free surface flow simulations reported in this article were done both with the direct solution method and the VOF approach. Typically the computational cost was considerable, with CPU times of the order of a few days on a state-of-the-art workstation. In these cases, the direct solution method was preferred. Specifically, the implementation of this method as available in the

commercial FVM flow solver CFX4 (AEA Technology) was used. As far as the VOF method is concerned, the commercial FVM solver CFD-ACE+ (CFDRC) was employed. In all corresponding simulations the piecewise-linear surface reconstruction scheme (PLIC) [5] was used. The contact angle of the two-phase system with the solid surface was considered as constant.

3 DROPLET FORMATION AND TRANSPORT BETWEEN FUNCIONALIZED SURFACES

The design of a gas/liquid reactor enabling surface-directed transport of droplets is shown in Fig. 1. The droplets span the margin between two parallel plates at a distance of 100 μm or smaller. On the surface of the plates there exist bands of comparatively high wettability (light gray) separated by bands of low wettability (dark gray). The droplets are driven by a gas flow parallel to the bands.

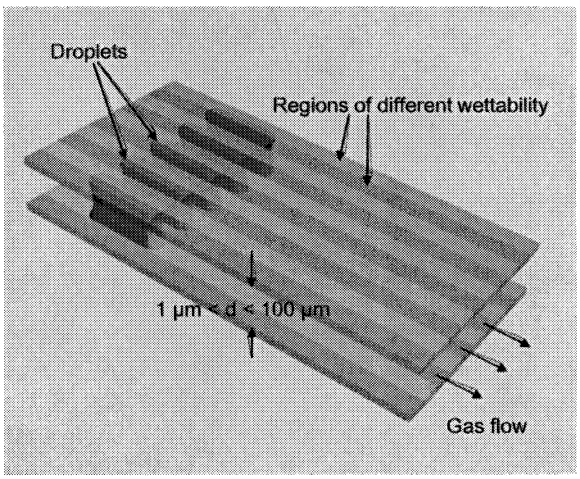

Fig. 1: Gas/liquid reactor with surface-directed flow.

An obvious advantage of such a design is the narrow residence time distribution of the liquid flow due to droplet transport. In addition to that, efficient heat and mass transfer from the gas and the surface to the liquid is expected due to recirculating flow within the droplets.

When developing a conceptual design for the reactor, two different problems have to be solved. The first problem is related to droplet creation, the second to droplet transport. Ideally, the reactor comprises structures allowing to create sufficiently small droplets between the plates. A set-up potentially qualifying to solve the first problem is shown in Fig. 2. Perpendicularly to the reactor plates, liquid inlets are arranged in such a way that the liquid stream meets the gas stream at an angle of 90°. The inlets are located in the middle of the bands of high wettability. In all the simulations reported, both types of bands have a width of 100 μm. The inlet holes for the liquid phases are squares of 50 μm side length. A parallel-plate distance of 50 and 100 μm was considered. Only a region containing half a band of each wettability was explicitly modeled, while symmetry boundaries limiting the computational domain accounted for the periodically repeating flow pattern. Optionally, a step structure of the same cross-sectional area as the liquid inlets with a height of half of the parallel-plate distance was modeled, as indicated in Fig. 2. As far as wettability is concerned, three different configurations were studied: ($\theta_1 = 20°$, $\theta_2 = 40°$), ($\theta_1 = 70°$, $\theta_2 = 110°$) and ($\theta_1 = 20°$, $\theta_2 = 140°$). θ_1 and θ_2 refer to the contact angles in the regions of high and low wettability, respectively. The liquid flow velocities considered are in the range between 0.1 and 1.0 m/s, the gas velocities are ranging from 1.0 to 20.0 m/s. The fluid properties of water and air at 20 °C and 1 atmosphere were used.

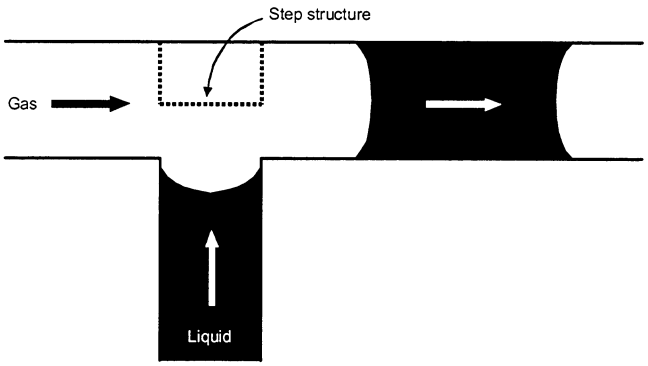

Fig. 2: Liquid inlet to the parallel-plates geometry.

In order to study droplet formation in the proposed geometry, simulations both with and without the step structure were performed. For this purpose a structured computational grid of approx. 40000 cells was defined.

For the simple geometry without the step structure, both parallel-plate spacings of 50 and 100 μm were considered. At comparatively low liquid velocities, the liquid jet emerging from the inlet hole is deflected before it reaches the upper plate due to the shear forces exerted by the gas stream. When the liquid velocity is increased to a certain point, the jet gets in contact with the upper plate. Then the liquid forms a lamella spanning the space between the two plates. However, for the geometries considered here such a lamella does not decay into droplets. The lamella stability clearly depends on the aspect ratio of its cross sectional area, from a certain aspect ratio on it might decay into droplets, i.e. separated volumes in contact with both surfaces. However, such high aspect ratio droplets are often unstable and are torn apart by the gas stream.

A solution to these problems is offered by the step structure sketched in Fig. 2. In the corresponding simulations a parallel-plate distance of 50 μm was considered. Fig. 3 shows the time evolution of the interface up to the point of droplet formation for contact angles of 20 and 40 degrees in adjacent bands. The step structure allows to access a different dynamical regime of the two-phase flow, since the minimum liquid velocity needed to reach the

upper wall decreases. As a consequence, droplets are formed and transported downstream by the gas flow.

Droplet transport can be regarded as a separate problem once the droplets are created. In this context, one of the most important questions is related to the influence of wetting properties on droplet dynamics. It should be pointed out that the corresponding CFD simulations only provide a course picture of the physics, as potentially relevant effects as dynamic contact angles or contact angle hysteresis [6] are not incorporated in the model.

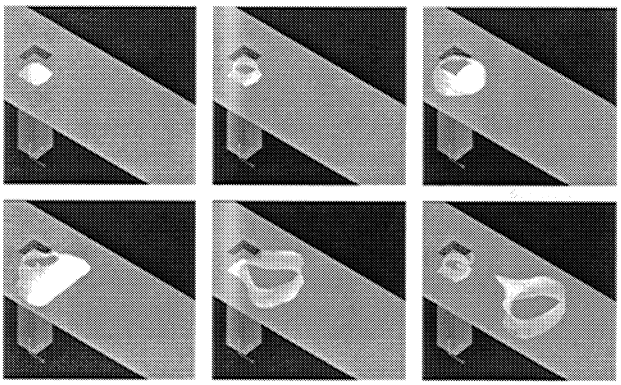

Fig. 3: Time sequence of droplet formation in the parallel-plates geometry.

For the case of rather small contact angles of 20° and 40°, droplets with a comparatively large transversal extension are observed in the simulations, as displayed in Fig. 4. The trailing edges of the droplets consist of long, thin structures which get detached as the droplets move. Hence, for small contact angles the simulations suggest that the interplay of wetting forces and drag forces exerted by the gas flow does not allow to keep the droplets fully intact while they are moving.

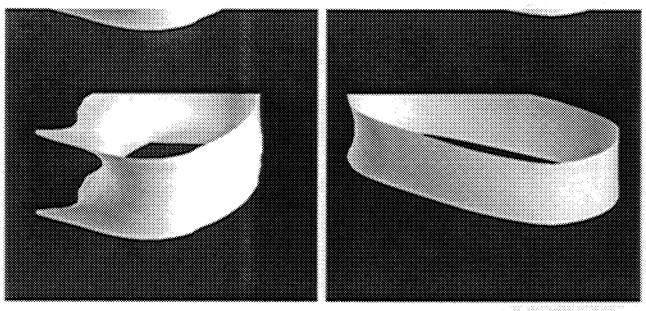

Fig. 4: Droplet shapes for high (left) and low (right) wettability of the surfaces.

The situation is different when the combination of larger contact angles (70° and 110°) is considered. In that case the droplets adopt an elongated shape, as they are repelled by the bands of low wettability (right side of Fig. 4). No detachment of small liquid volumes is observed and the droplets keep fully intact while they are moving.

A series of simulation runs with different gas velocities showed that there is a critical gas velocity below which the droplets are transported without being disrupted. As an example, the droplet shown in Fig. 5 (only one half of the droplet displayed) is strongly deformed and finally fragmented into two pieces at a gas velocity of 20 m/s. At a velocity of 2 m/s, the same droplet stays intact. For the corresponding simulations contact angles of 20° and 140° were assumed.

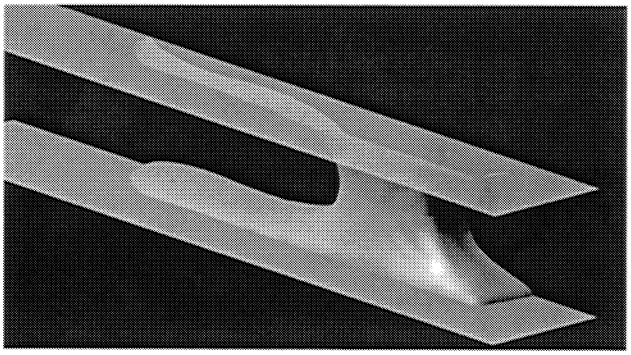

Fig. 5: Strongly deformed droplet at a gas velocity of 20 m/s.

4 BUBBLE FLOW IN CAPILLARIES

With the micromixing technology developed at IMM it is possible to create dispersions with a very narrow bubble size distribution. When such dispersions are transported through a narrow capillary, the bubbles form a regular arrangement similar to a dense packing of spheres. In such a way it is possible to achieve bubble volume fractions in the range of 70 %, close to the densest packing of about 74 % according to Kepler's theorem.

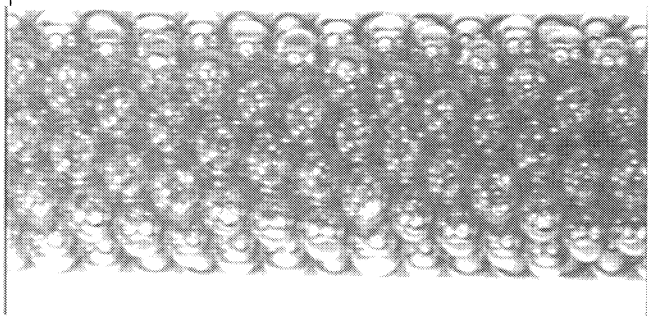

Fig. 6: Regular arrangement of bubbles flowing through a capillary.

The phenomenon is illustrated in Fig. 6, which shows the flow of nitrogen bubbles surrounded by a mixture of 65 % glycerol, 35 % water and 0.01 mol/kg SDS in a capillary of 2.7 mm inner diameter. From observation of the flow patterns it is suggested that no relative motion between the bubbles exist, i.e. the foam moves through the capillary

while maintaining its structure. This observation is strongly supported by experiments on the dispersion of concentration tracers. For this purpose an aqueous tracer dyed with water blue was added to a regular foam consisting of water, 0.01 mol/l SDS and nitrogen. Then the foam was transported through a capillary of 1.5 m length and 2.7 mm inner diameter at a total flow rate of 40 ml/h. It was found that the temporal broadening of the tracer signal was about 30 times smaller than the residence time of the flow, thus indicating very small hydrodynamic dispersion.

Clearly, such regular flow patterns open up promising perspectives for gas/liquid reactors. The residence time distribution allows for a well-defined contact time in gas/liquid reactions. Furthermore, the high surface-to-volume ratio enables an efficient mass transfer.

In order to study bubble flow in capillaries, a 2D simulation model was set up. The spatial resolution of the complicated gas/liquid interface requires a comparatively fine mesh. As the liquid layers separating two adjacent bubbles become very thin at high gas volume fractions - thus requiring very small grid cells - a volume fraction of only 49 % was considered. For the solution of the volume fraction equation, the direct method in combination with the surface-sharpening algorithm was used, thus eliminating the severe CFL number limits of the VOF algorithm. One of the problems related to the direct method is the artificial diffusive decay of thin liquid layers in addition to convective decay. The combination of these two effects usually causes a rapid coalescence of the bubbles which is somehow attenuated for high-viscosity liquids with low surface tension.

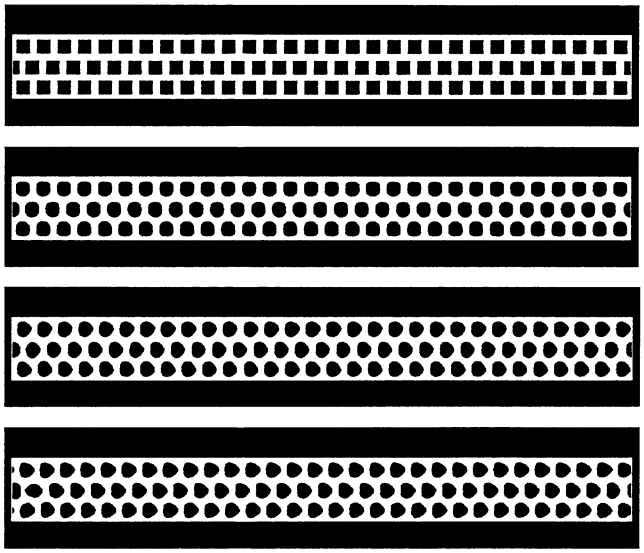

Fig. 7: Simulation of bubble flow in a 1 mm capillary.

The simulation results for a capillary of 1 mm diameter are shown in Fig. 7. The material properties of air and water were used, except that the water viscosity was increased by a factor of 10 and the surface tension was chosen 10 mN/m. A body force acting in the horizontal direction was modeled in order to drive the fluids. The structured computational grid comprises about 35000 cells. By action of surface-tension, the initially square-shaped bubbles assume a rounded shape. When the bubbles start to move, they assume an asymmetric shape with a cusp in flow direction (a zero velocity was initialized). Clearly, the staggered arrangement of the bubbles is maintained while they are moving. This indicates that the foamy structure is kept intact, in qualitative agreement with the experiments. After about 1 ms, bubble coalescence is observed (not shown), thus preventing to draw any further conclusions on the velocity profile of the flow.

These first simulations only give a comparatively coarse picture of ordered bubble flows in capillaries and require further studies. In future investigations the computational model will have to be refined in order to suppress artificial bubble coalescence.

5 SUMMARY AND CONCLUSIONS

Two different concepts of high-performance gas/liquid reactors have been investigated using CFD methods. The first concept is based on droplet transport between functionalized surfaces. Based on the simulations a simple geometry was suggested allowing for droplet formation within the parallel-plate geometry. Furthermore, the influence of wettability of the surface and gas velocity on the droplet dynamics was investigated. Dynamical regimes showing a disruption of the droplets were identified. The second concept is based on regular arrangements of bubbles flowing through capillaries. Experiments indicated that such foams are kept intact while being transported through the capillary. Corresponding simulations support the experiments and show that the bubbles keep their staggered arrangement while moving. Both concepts promise to open up new directions towards high-performance gas/liquid microreactors with a narrow residence-time distribution and efficient mass transfer between the phases.

REFERENCES

[1] V. Hessel, W. Ehrfeld, K. Golbig et al., Proc. of IMRET3, Springer-Verlag, 526-540, 2000.

[2] S. Hardt, F. Doffing and H. Pennemann, Proc. of MSM2002, Computational Publications, 54-57, 2002.

[3] B. Lafaurie, C. Nardone, R. Scardovelli et al., J. Comp. Phys. 133, 134-147, 1994.

[4] C.W. Hirt and B.D. Nichols, J. Comp. Phys. 39, 201-225, 1981.

[5] D.B. Kothe, W.J. Rider, S.J. Mosso et al., AIAA Paper 96-0859, 1996.

[6] P.G. de Gennes, Rev. Mod. Phys. 57(3), 827-863, 1985.

ACKNOWLEDGEMENT

This work was supported by the European Commission, grant number G1RD-CT-2000-00469 (KEMiCC).